

NSRL Beam Characterization Study

I. Chiang, A. Rusek

December 2005

Collider Accelerator Department
Brookhaven National Laboratory

U.S. Department of Energy

USDOE Office of Science (SC), Nuclear Physics (NP) (SC-26)

Notice: This technical note has been authored by employees of Brookhaven Science Associates, LLC under Contract No. DE-AC02-98CH10886 with the U.S. Department of Energy. The publisher by accepting the technical note for publication acknowledges that the United States Government retains a non-exclusive, paid-up, irrevocable, world-wide license to publish or reproduce the published form of this technical note, or allow others to do so, for United States Government purposes.

DISCLAIMER

This report was prepared as an account of work sponsored by an agency of the United States Government. Neither the United States Government nor any agency thereof, nor any of their employees, nor any of their contractors, subcontractors, or their employees, makes any warranty, express or implied, or assumes any legal liability or responsibility for the accuracy, completeness, or any third party's use or the results of such use of any information, apparatus, product, or process disclosed, or represents that its use would not infringe privately owned rights. Reference herein to any specific commercial product, process, or service by trade name, trademark, manufacturer, or otherwise, does not necessarily constitute or imply its endorsement, recommendation, or favoring by the United States Government or any agency thereof or its contractors or subcontractors. The views and opinions of authors expressed herein do not necessarily state or reflect those of the United States Government or any agency thereof.

Beam Characterization Studies at NSRL

Introduction

The heavy ions fragment and scatter in the stripping foil, vacuum window, ionization chambers and in the air along the beamline. This means a beam that is intended to be Fe-56 can have components from $Z=1$ to $Z=26$ and everything in between. Although this is not much of a concern for most users who are primarily concerned about total dose and dose rate, any user interested in effects of tracks will be very concerned. The goal of this study is to characterize the particles in the beam, as a function of Z , so that users will know what tracks are contributing to the total dose, and how the dose is delivered.

We measured the fragmentation by placing a combination of scintillators and Cherenkov counters directly in the beam and also off the primary beam axis. Beam particles are identified by comparing the energy loss (dE/dX) in thin and thick scintillators with the light output of a Cherenkov radiator that the particles traverse.

Detector

The fragmentation detectors are composed of a variety of scintillators and Cherenkov radiators mounted inside a light-tight reflective tube which acts as an air light guide. Two trigger scintillators are $1.5\text{cm} \times 1.5\text{cm} \times 0.1\text{cm}$ in size. A thick scintillator of dimensions $1.5\text{cm} \times 1.5\text{cm} \times 1.0\text{cm}$ generated lots of light for good energy loss measurements. A Cherenkov radiator made of UVT plastic ($1.5\text{cm} \times 1.5\text{cm} \times 0.5\text{cm}$) with a frosted surface to scatter the Cherenkov light was also used as a track detector. For some of the data taking, a plastic scintillator veto counter was used. The dimensions of the veto counter are $2.0\text{cm} \times 2.0\text{cm} \times 0.5\text{cm}$ with a cylindrical hole of diameter 1.0cm in the center. The veto counter was used to ensure that tracks did not leave the fragmentation counter through the side. Since this did not appear to be a significant problem with the trigger counter configuration we used, the veto counter was not routinely included in the trigger.

The detector has four phototube holders mounted in a single rigid frame that rides on the rails in the target room and allows the PMTs to be centered underneath the beam. The PMTs are 2" tubes. Each PMT is mounted inside a long Aluminum tube with a rectangular window cut out of it front and back to allow the beam to pass through without additional fragmentation. The windows are blacked out to protect the PMTs, and the tubes are lined on the inside with Aluminized Mylar to reflect light generated in the scintillators or Cherenkov radiator towards the PMTs. This avoids the use of Lucite light guides that could produce unwanted Cherenkov light pulses.

Each PMT signal is transmitted ~ 300 feet to the NSRL control room where it is split in a passive splitter. Half the signal is sent to a discriminator to generate a digital pulse for triggering and for TDC input. The other half is delayed $\sim 100\text{ns}$ before entering a Dual Range QDC (CAEN V965N).

The trigger for the data acquisition was formed from the coincidence of the front and back trigger scintillators, $T1 * T2$. The Trigger PMTs are operated at -1700 volts allowing the discriminators to fire when the thin scintillators were traversed by a singly charged track like a proton. The Cherenkov and Scintillator counters operated at different voltages depending on the beam under study in order to keep from saturating the QDC for fully stripped ions while retaining resolution for singly charged tracks. The coincidence of $T1 * T2$ is used to generate a 150ns wide Gate for the QDC. This trigger signal also started a Gate Generator used to provide $\sim 1\text{ms}$ dead

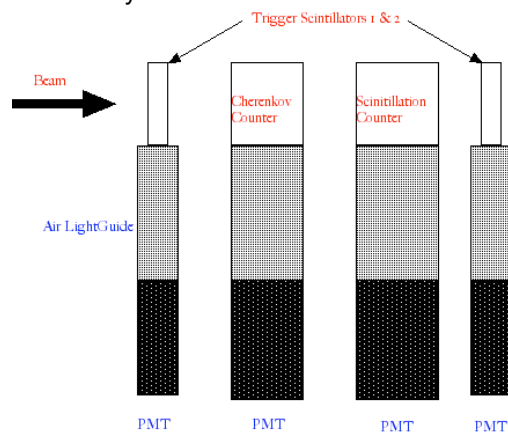


Figure 1: Schematic layout of the NSRL Fragmentation Detector.

time for each trigger to keep from crashing the data acquisition system (DAQ). The DAQ is part of the PET system, reading out the QDC and TDC on every trigger. A Scaler was added to the DAQ, with a 1kHz pulser input to the scaler, and a Clear signal provided at the Booster Start-of-Spill. The scaler is used to study any dependence on the spill structure or extracted beam momentum that varies by ~0.5% throughout the spill.

For some running we exchanged the Cherenkov counter for another scintillator, at times when the beam velocity dropped close to or below the Cherenkov threshold such as the 300MeV Silicon running.

Data Taking

Every effort was made to ensure that the beam transport was substantially the same as during normal running so that we could apply whatever we learned about beam characterization and fragmentation to the NASA running conditions. But in order to take data with this detector, the beam intensity had to be reduced to very low levels; typically a few thousand triggers per ~300ms spill. This is accomplished with help from the Tandem cutting back on the intensity by two orders of magnitude from normal running. The chopper was used to cut back the intensity even further. Finally the collimator was used to bring the rate down to a level we could run with. The high-gain ionization chamber was used to study the beam profile as the intensity was reduced to verify that the transport stayed the same.

Most data taking took place with the detector at the downstream end of the NASA beamline, after the beam passes through ~8m of air and 0.7cm of glass mirror in the camera, both of which contribute to fragmentation. Some data were taken with 4-10cm of high density polyethylene in place to enhance the fragmentation.

Fragmentation studies were conducted using beams of Fe, Si, O, and H at kinetic energies of 300MeV and 1000MeV. The challenge was to observe the energy loss of the unfragmented ion as well as the secondary peaks formed by all the fragments down to protons. This requires a large dynamic range since the Cherenkov light output scales like Z^2 meaning a Fe-nucleus gives 676 times the light output of a proton.

We ran the trigger counters at 1700 volts with discriminator settings of 50mV for good triggering efficiency for singly charged tracks. The gains of the Cherenkov counter and scintillator counter were adjusted to place the Fe peak near the end of the QDC range.

Below are some of the fragmentation spectra taken along with a brief description of the conditions.

Date	Ion – MeV	Configuration	Trigger	Comments
26-Oct-05	Fe – 1000	Veto-Scint-T1-T2	T1*T2	Study begins
07-Nov-05	Fe – 1000	T1-C-Veto-T2	T1*T2*V	Veto in trigger
08-Nov-05	Fe – 1000	T1-C-Veto-T2	T1*T2*V T1*T2*V*C	Prescale high rate trigger/add deadtime/add high threshold C
09-Nov-05	Fe – 1000	T1-C-Veto-T2	T1*T2	Vertically Smaller beam
10-Nov-05	Fe – 1000	T1-C-Veto-T2	T1*T2	
11-Nov-05	H – 1000	T1-C-Scint-T2	T1*T2	Replaced veto with scintillator
14-Nov-05	Fe – 1000	T1-C-Scint-T2	T1*T2	Detector off beam center by 137cm
14-Nov-05	H - 1000	T1-C-Scint-T2	T1*T2	Data taking at High Beam Rate
15-Nov-05	H - 1000	T1-C-Scint-T2	T1*T2	Raised C HV to 2700
16-Nov-05	O - 1000	T1-C-Scint-T2	T1*T2	Returned C HV to 1750, Oxygen
17-Nov-05	Si – 1000	T1-C-Scint-T2	T1*T2	Looking at Silicon
18-Nov-05	Si – 300	T1-C-Scint-T2	T1*T2	C HV at 2700
18-Nov-05	Si – 300	T1-C-Scint-T2	T1*T2	C HV at 1750
18-Nov-05	Si – 300	T1-Scint-Scint-T2	T1*T2	Replaced C with thin scintillator

Table 1: List of Fragmentation studies conducted during the NSRL-7 run.

Observing the components of the beam

The effects of fragmentation (and scattering) are of little importance to users who are concerned only with dose measurements. Most NSRL users assume that it is only the total dose or dose rate that needs to be accounted for. A few users are interested in studying the effects that are track-dependent, and for these users it is important whether the dose is delivered by a $Z=26$ ion or a singly charged particle like a proton, or something with intermediate Z .

We made use of the variation in dE/dX in plastic scintillator and Cherenkov light with Z to separate out the charge states of different components of the beam. Our goal was to characterize the beam delivered to the NSRL target. Due to the limited acceptance of the beam transport, it is assumed that only a single species of ion can be successfully transported to the target. So any fragmentation we observe takes place in the material in the beam line. This includes the vacuum window that is 15 mils (0.381mm) thick Aluminum, about 5 meters of air, and several ion chambers, typically four. Each ion chamber is composed of 5 mils (0.018 g/cm^2) kapton, $68 \mu\text{m}$ (0.061 g/cm^2) Copper, $0.040 \mu\text{m}$ (0.077 mg/cm^2) gold, and 4 cm of Nitrogen gas.

Fragmentation can be enhanced by inserting high density polyethylene from the binary filter into the beam. In this run we made use of 4cm and 10cm at various times. The fragmentation measurements made with polyethylene in the beam show a fragmentation rate for most ion species that is close to expectations based on total cross sections for pp scattering and the assumption that the scattering cross section scales like $A^{0.8}$. This assumption is consistent with neutron cross sections published by the NNDC¹ for $\sigma(nZ \rightarrow X)$. In addition to fragmentation, beam components can come from elastic and inelastic scattering processes in the material in the beam.

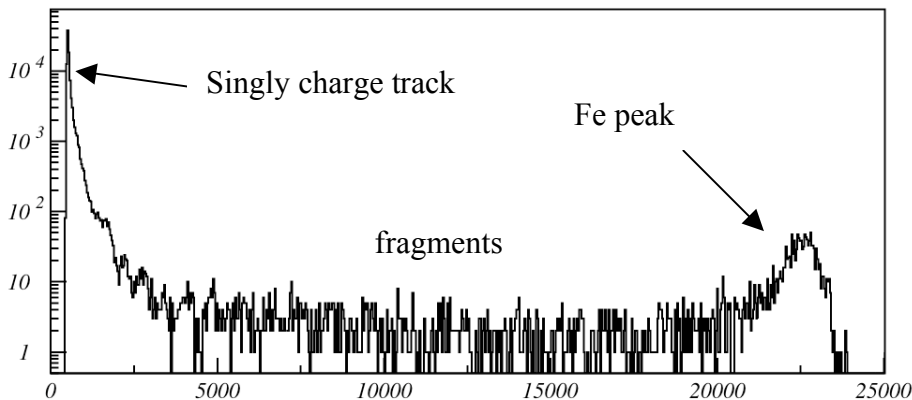


Figure 2: Fragmentation distribution from 1000 MeV Fe ions measured with a Cherenkov radiator. The horizontal axis is in QDC bins (25fC/bin).

The asymmetric peak near 23000 is due to the Fe ions, with the tail on the low side due possibly to fragments with Z near 26. Singly charged tracks like protons can be seen in the region near 500. Some of the singly charged tracks may be pions formed by Fe interactions in the air, or vacuum windows. For these running conditions, the QDC pedestal was typically in bin 430 for the Cherenkov counter and had an RMS width of ~ 5 bins. A singly charged track would appear ~ 30 bins above pedestal. This calibration was tested with numerous proton runs.

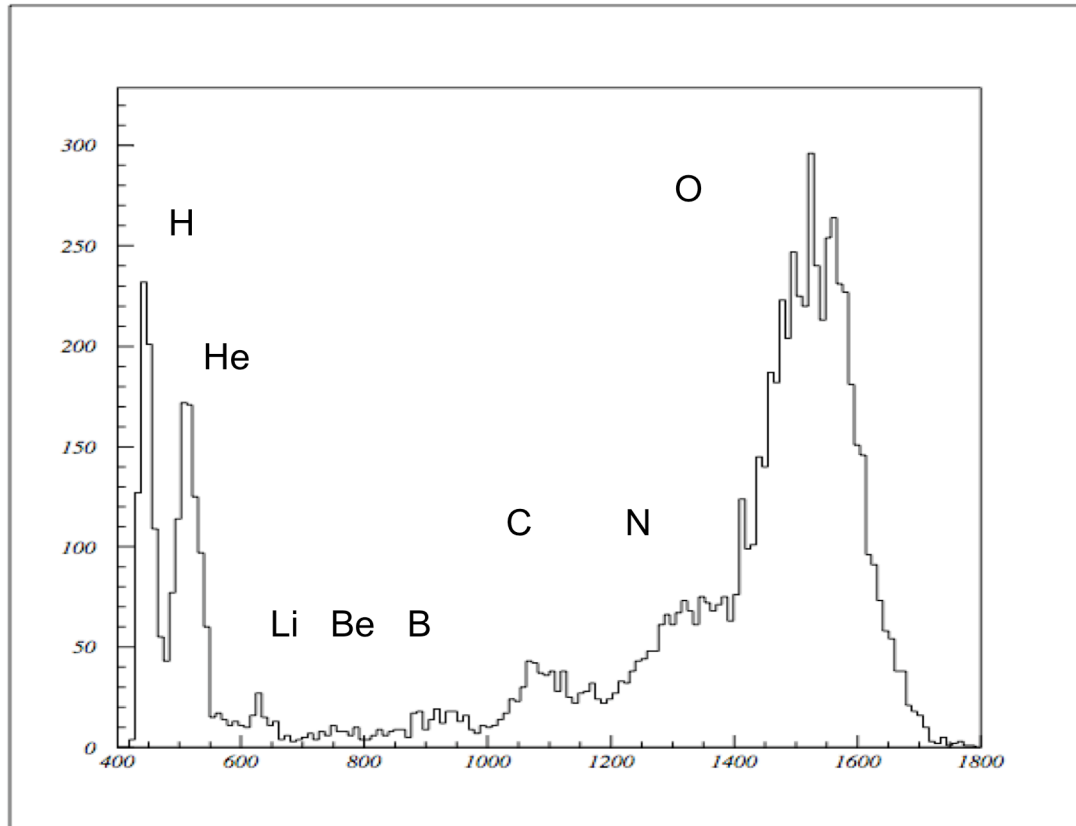


Figure 2: 1000 MeV Oxygen fragmentation spectrum produced when the beam passes through 10 cm of high density polyethylene, as observed with a Cherenkov counter. The peaks for $Z=1$ through $Z=8$ can be easily identified.

The detector operated at the same gain for Oxygen as for Iron. In the 1000 MeV Oxygen running it is possible to isolate fragmentation peaks from all 8 charge states, made easier by adding 10cm of high density polyethylene in the path of the beam to enhance fragmentation. The location of the peaks is in reasonable agreement with the expectation that the light output of a Cherenkov Counter scales with Z^2 , although there is some evidence of non-linearity for the largest pulse heights that may be due to saturation of the phototube base.

The ratio of $Z=1$ tracks to the $Z=Z(\text{beam})$ tracks is much smaller for O than for Fe, even though the added polyethylene should enhance fragmentation. In the Fe spectrum there is not as much clear evidence for many lower Z fragments. The $Z=1$ tracks are thus most likely to be a mixture of secondary particles like pions and their decay products. The cross section for pion production scales roughly like $A^{0.8}$ at these energies, predicting nearly five times as many pions per beam particle for Fe than for O, in agreement with observations.

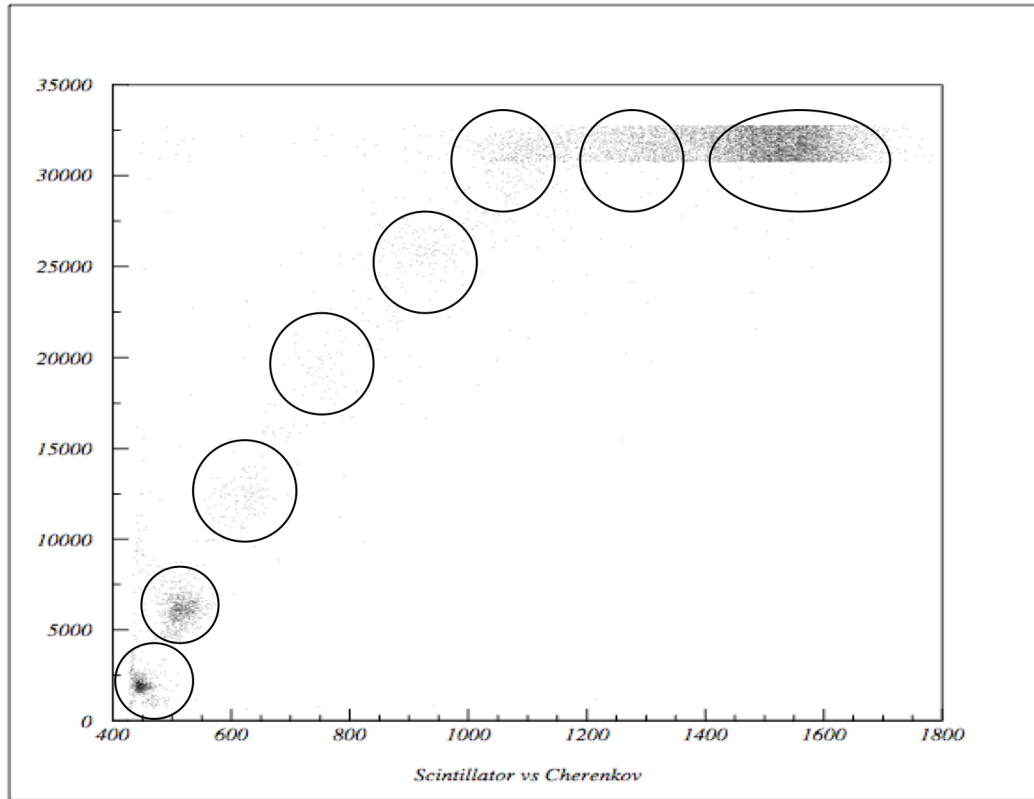


Figure 1: Comparison of scintillator and Cherenkov response to 1000MeV Oxygen. The vertical axis is the scintillator QDC and the horizontal axis is the Cherenkov QDC. All axes are in QDC bins (25fC/bin).

By comparing the response of the thick scintillator and the Cherenkov counter, it is easy to pick out the regions corresponding to each value of Z . At these operating voltages, the scintillator response saturated the QDC (which returns a value in the range 30000 and 33000 when saturated in this way) for $Z=7$ and 8.

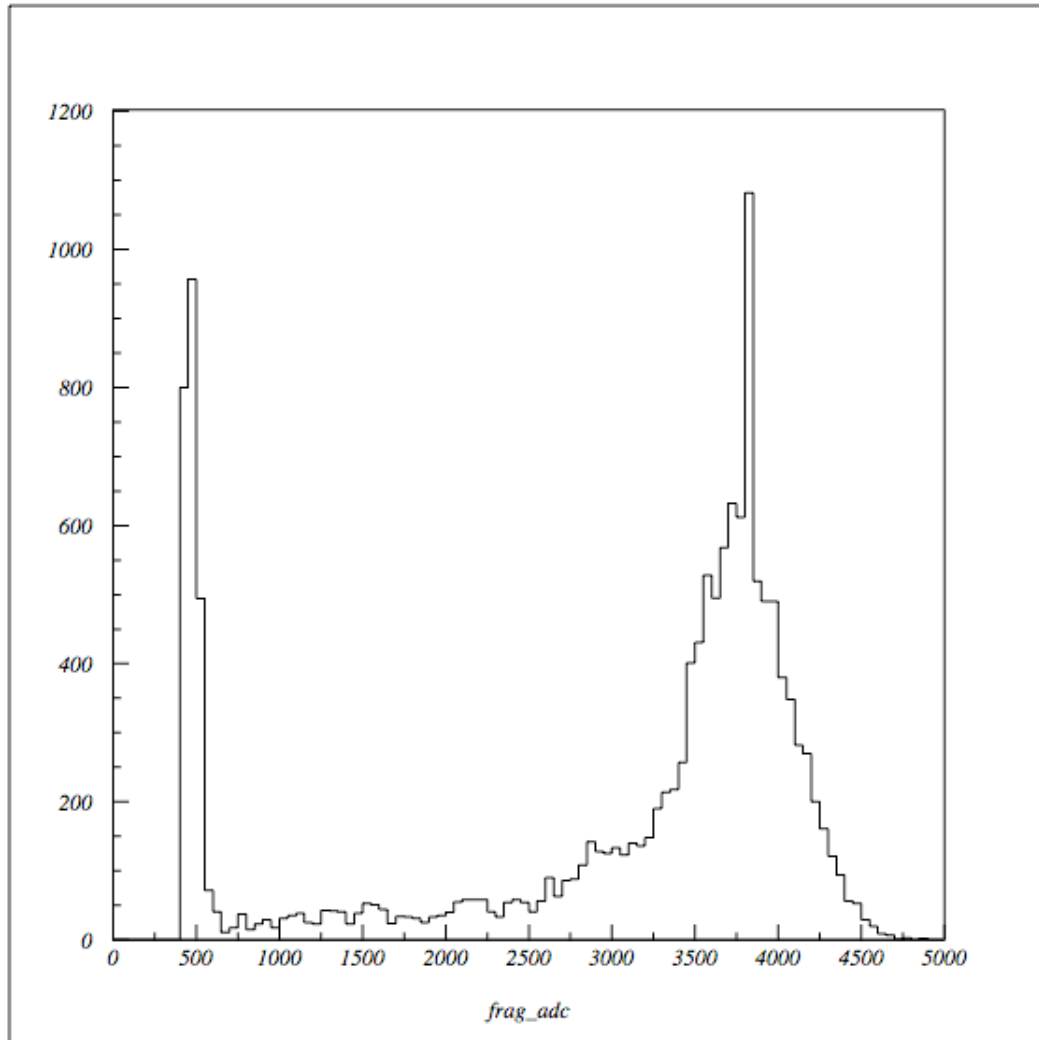
1000MeV Silicon Spectrum

Figure 2: 1000 MeV Silicon fragmentation spectrum. Horizontal axis is in QDC bins (25fC/bin).

The fragmentation spectrum for Silicon shows the same features, in general, as does Oxygen. The same level of fragmentation is observed, including the low Z region. In Figure 4, the Z=1 and Z=2 peaks are not resolved, so a blow-up of the low-energy region is shown in Figure 5. The QDC pedestal is at bin ~430 with an RMS width of ~5 bins, so it is possible that the Z=1 peak may include some small fraction of pedestal events as well. (The spike near 3750 is due to the change of range in the dual-range QDC.)

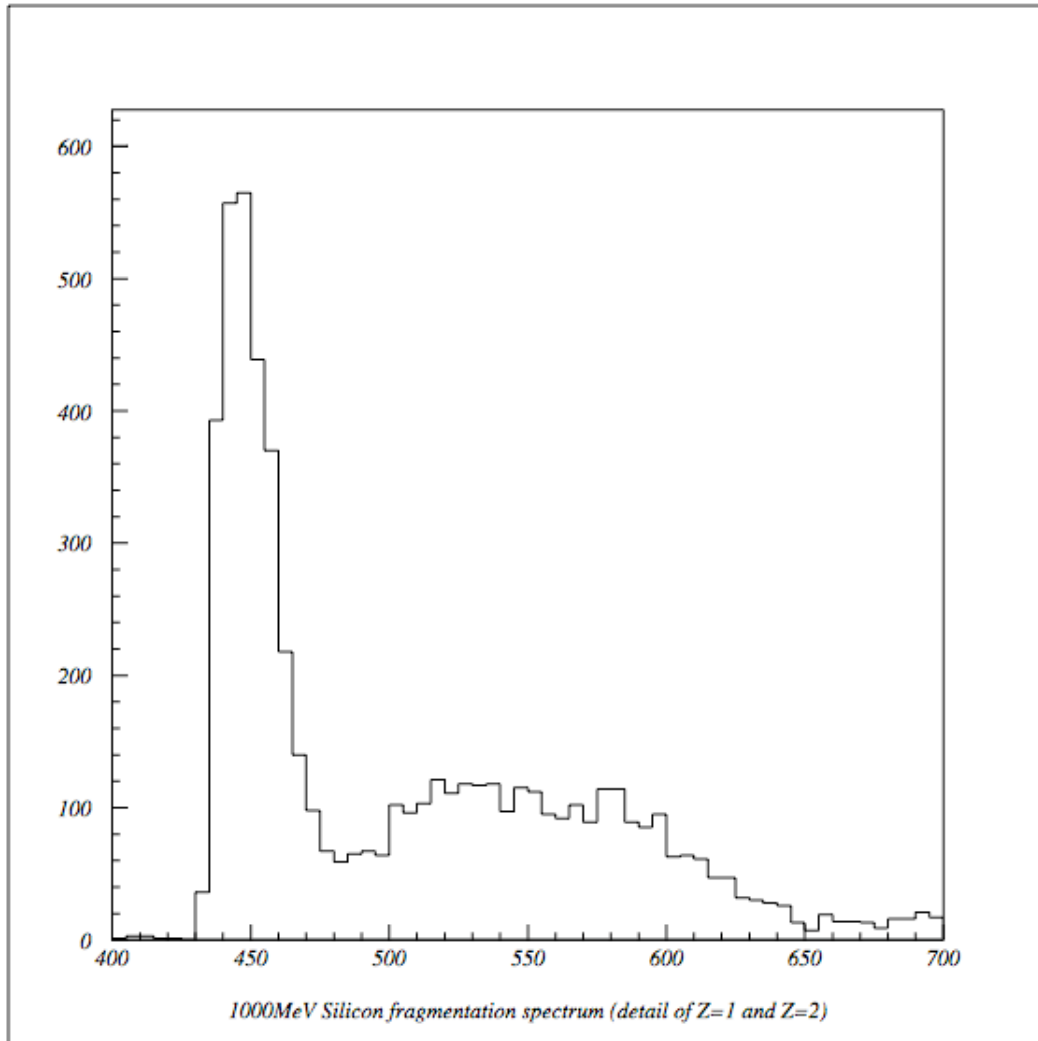


Figure 3: Detail of the Silicon fragmentation spectrum for $Z=1$ and $Z=2$ fragments. The horizontal axis is in QDC bins (25fC/bin). Pedestal is in bin 430.

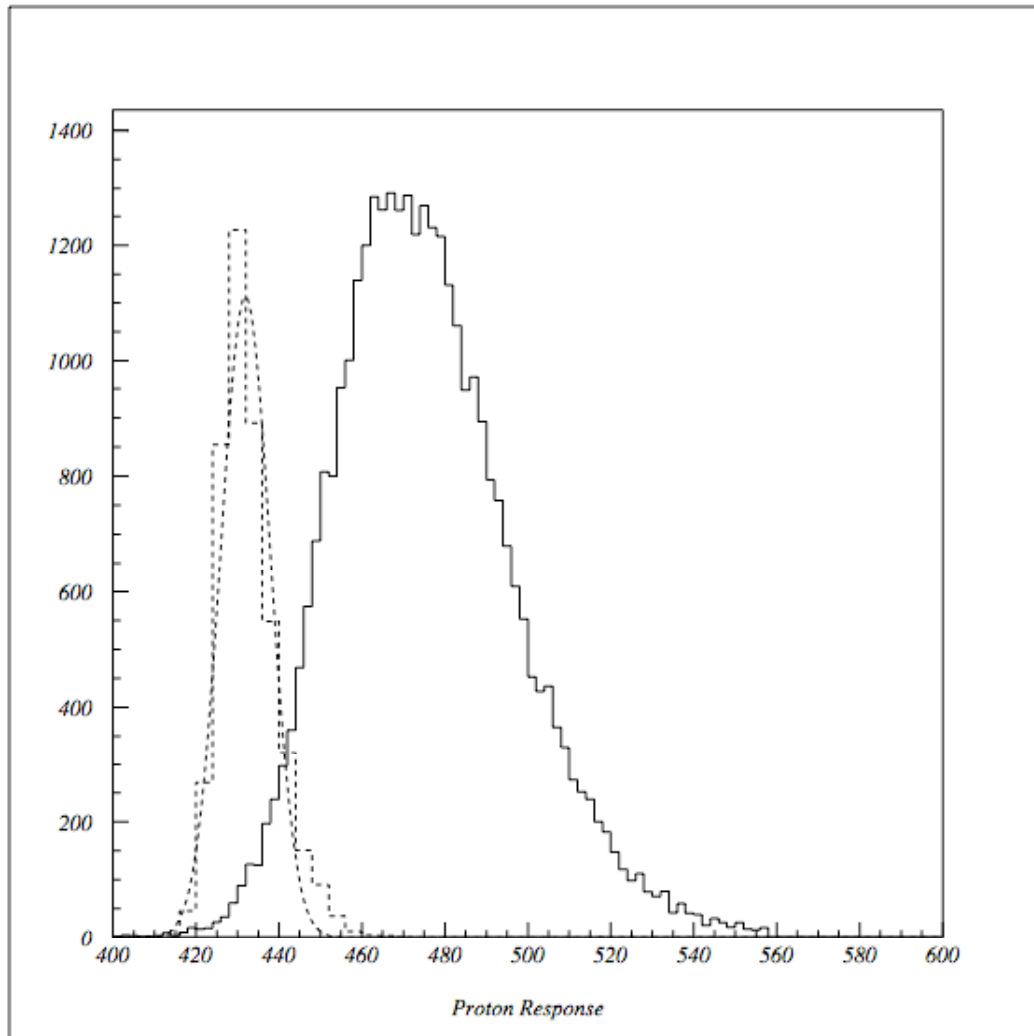


Figure 4: Cherenkov counter response to 1000 MeV protons. Also shown (dashed) is the QDC pedestal distribution taken at the same time under running conditions but with the signal out of the QDC gate. The horizontal axis is in QDC bins (25fC/bin).

The proton running confirms the calibration of the Cherenkov counter, giving confidence that the singly charged tracks can be observed above background with the same detector configuration used to measure the Fe beam.

Further study is needed to fully understand the make-up of the singly charged peak in the Fe (and O and Si) data.

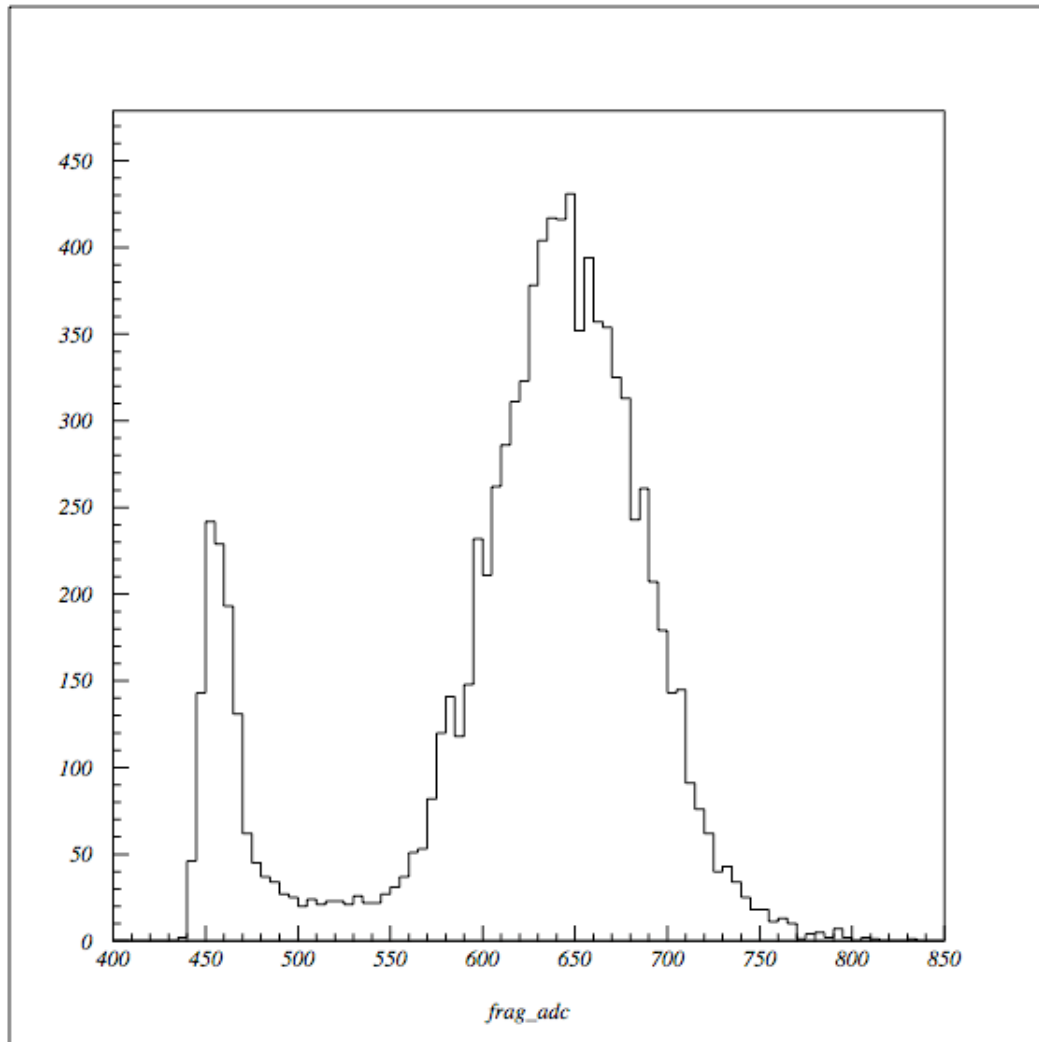


Figure 5: 300 MeV Silicon fragmentation spectrum.

For the 300MeV Silicon running, the light out of the Cherenkov counter is greatly reduced. This is due to the fact that at a kinetic energy of 300MeV, the velocity of the Si ions are barely above the Cherenkov threshold.

¹ National Nuclear Data Center results for $n Z \rightarrow X$, where Z is a nucleus from H to Fe; see <http://www.nndc.bnl.gov/>.